Obat: Jurnal Riset Ilmu Farmasi dan Kesehatan
Volume. 3 Nomor. 6 November 2025
e-ISSN : 3031-0148, p-ISSN : 3031-013X, Hal. 288-301
DOI: https://doi.org/10.61132/obat.v3i6.1943
Tersedia: https://journal.arikesi.or.id/index.php/OBAT

Synthesis of Vanadium Pentoxide (V_2O_5) by Green Method Using Olive Oil as A Reducing Agent and Study of its Physical Properties

Ahmed Saleh Yaseen [1*], Yosef Othman Homeda[2], Mohammad M. Al-Tufah[3], Mutlak Saud Khalaf[4] , Mohannd Faisal Shareef [5]
[1,2,5] Tikrit University, College of Education for Pure Science, Department of Chemistry, Tikrit, Iraq.
[3] Directorate of Education, Kirkuk, Ministry of Education, Iraq.
[4] Ghatfan Preparatory School for Boys, Ministry of Education, Salah Aldin, Iraq.
Email: ahmed.s.yaseen@tu.edu.iq [1], yosef.a.homeda@tu.edu.iq [2] , Mohamadmd282@gmail.com [3] , mtlkswdalljy@gmail.com [4] mohannad.f.shareef@tu.edu.iq [5]
*Author Correspondence: ahmed.s.yaseen@tu.edu.iq

Abstract. *This study reports the green synthesis of vanadium pentoxide (V_2O_5) using virgin olive oil as a natural and environmentally benign reducing agent. The approach aims to minimize the environmental impacts associated with conventional synthesis routes. Structural and physicochemical characterizations confirmed the successful formation of nanoscale V_2O_5. X-ray diffraction (XRD) analysis indicated an average crystallite size of approximately 16.57 nm, evidencing high crystallinity. Fourier-transform infrared spectroscopy (FTIR) revealed characteristic V=O and V–O–V vibrations with bands associated with physisorbed water, confirming the correct oxide framework. Field-emission scanning electron microscopy (FE-SEM) showed irregularly shaped nanoparticles with a representative particle diameter of ~32.62 nm. Brunauer–Emmett–Teller (BET) and Barrett–Joyner–Halenda (BJH) analyses yielded a specific surface area of 10.817 m^2/g, a total pore volume of 0.024277 cm^3/g, and a broad mesoporous distribution (20–90 nm). Energy-dispersive X-ray spectroscopy (EDX) confirmed the purity of V_2O_5 with weight fractions of V (69.40%) and O (30.60%), consistent with the stoichiometric composition. Overall, the results demonstrate the effectiveness of olive oil as a green reducing agent for preparing nanoscale V_2O_5, which is promising for catalysis, energy storage, sensors, and clean-energy applications.*

Keywords: *Catalysis; Green Chemistry; Nanomaterials; Vanadium Pentaoxide; X-Ray Diffraction.*

1. INTRODUCTION

In the early nineteenth century, vanadium oxide was discovered and isolated from its natural ores . After that, several studies were conducted to prepare different vanadium oxides, which attracted researchers to study their physical properties for use in various applications. Vanadium pentoxide (V_2O_5) is a yellow crystalline solid with the chemical formula V_2O_5. Also known as vanadium pentoxide, it is a strong oxidizing agent and is used as a catalyst in many chemical reactions. This oxide is one of the important oxides found in nature. It occurs in rare minerals, most notably patronite, from which vanadium oxides are extracted. This oxide is also found in carnotite and vanadate. The importance of studying the presence of vanadium oxide lies in understanding the vanadium cycle in the Earth's crust and exploring its natural sources, which are essential to meet growing industrial demand. Because of the physical properties of vanadium pentoxide make it suitable for use in energy storage, catalysis, and electronic devices. Vanadium pentoxide can be synthesized using chemical and physical methods, including thermal reactions and the use of environmentally harmful chemicals. The concept of green chemistry has emerged as one of the main pillars for reducing pollution and reducing the use of toxic materials in the chemical industry, with the global trend towards developing environmentally friendly production methods. One of the most prominent scientific studies in

Naskah Masuk: 17 September 2025; Revisi: 21 Oktober 2025; Diterima: 28 November 2025; Terbit: 30 November 2025

recent years has been conducted by Zhang et al. on methods for preparing vanadium pentoxide (V_2O_5) using environmentally friendly methods, in line with the principles of green chemistry (9). Reducing agents from plant extracts were then used to synthesize V_2O_5 nanoparticles under mild conditions and without the use of toxic organic solvents. The study conducted by Kumar et al. also suggested the possibility of using biopolymers such as chitosan as a catalyst in the preparation of V_2O_5 in a way that reduces the amount of waste generated. In another study, Wang et al. (2020) reviewed preparation methods using microwave-assisted synthesis, which proved to be efficient in reducing energy consumption and reaction time compared to conventional thermal methods. Given the importance of vanadium resources, they can be extracted from industrial waste (such as spent catalysts), recycled, and converted into V_2O_5 sustainably and efficiently. Together, these studies demonstrate that advances in the green synthesis of V2O5 not only improve industrial performance but also achieve sustainable development goals and reduce environmental impact. Vanadium V oxide (V_2O_5) is widely used as a catalyst in the glass, ceramics, and battery industries. With the increasing demand for vanadium oxide, it has become necessary to develop synthesis methods based on green chemistry principles, which reduce energy consumption, minimize toxic waste, and use environmentally friendly solvents and raw materials. In our work aimed at the synthesis of vanadium pentoxide (V2O5) using virgin olive oil as a natural reducing agent within the green synthesis approach, while evaluating the physical properties of the prepared material.

2. MATERIALS AND METHODS

Analytical-grade vanadyl sulfate ($VOSO_4$) was obtained from Sigma Al Daraj; virgin olive oil was sourced from a local producer. Deionized water was used in all steps.

Preparation of the Standard Solution

A precisely weighed quantity of vanadyl sulfate ($VOSO_4$) was introduced into a suitable volume of deionized water, after which the mixture was subjected to gentle heating in the range of 50–60 °C. This controlled heating step was applied to accelerate the solubilization process and to guarantee the complete dissolution of the salt without leaving any undissolved residues. Once the dissolution was achieved, the compound dissociated in the aqueous medium, releasing vanadyl cations (VO^{2+}) together with sulfate anions (SO_4^{2-}). The dissociation mechanism can be represented by Equation (1), which illustrates the ionic species present in the solution following the solvation of $VOSO_4$.

$$VOSO_4 \rightarrow VO^{2+} + SO_4^{2-} \quad (1)$$

Addition Raw Olive Oil

Olive oil was gradually introduced into the reaction medium at a controlled volumetric ratio of 1:5 (oil to solution), in order to maintain homogeneity and regulate the interaction between the organic and inorganic phases. The chemical composition of olive oil is dominated by triacylglycerols, which serve as the primary structural and functional constituents of this natural lipid. When the reaction system is heated to approximately 85 °C in the presence of both water molecules and vanadyl sulfate species, the triacylglycerols undergo partial hydrolysis. This process results in the cleavage of ester bonds, leading to the release of free fatty acids along with glycerol fragments. The general scheme of this hydrolytic transformation, which highlights the breakdown of triacylglycerol units into their fundamental components under the described conditions, is outlined in Equation (2).

$$C_{18}H_{34}O_2 + VOSO_4 \rightarrow C_{18}H_{32}O_2 + VO(SO_4)_2 + H_2O \quad (2)$$

Hydrothermal Reaction

The prepared mixture was carefully transferred into a ceramic reaction vessel, chosen for its stability and resistance to high-temperature treatments. The system was then subjected to thermal processing by heating at 200 °C for a continuous duration of 24 hours, ensuring sufficient time for the chemical transformation to proceed to completion. Under these controlled thermal conditions, the precursor species undergo hydrolysis and condensation, ultimately yielding vanadium hydroxide as an intermediate phase.

$$VOSO_4 + C_{18}H_{32}O_2 \rightarrow H_2O + C_{18}H_{34}O_2 + VO(SO_4)_2 \quad (3)$$

Separation and Wash the Product

Upon completion of the thermal reaction, the ceramic vessel was gradually cooled down to ambient (room) temperature in order to avoid sudden thermal stress and to allow the system to equilibrate. The solid product that precipitated during the reaction was then carefully separated from the liquid phase by means of vacuum-assisted filtration using nano-porous filter paper, which provides high selectivity and efficiency in retaining fine particles. Following the filtration step, the collected precipitate was repeatedly rinsed with deionized water. This washing process was essential for removing any traces of residual olive oil, unreacted precursors, and other soluble by-products. Additionally, multiple washing cycles ensured the adjustment of the surface environment of the precipitate, effectively neutralizing the pH and improving the purity of the obtained material for subsequent characterization and analysis.

Dryeration and Calcination

In the initial stage of the process, the olive oil does not directly participate as a reactant in the main chemical transformation; instead, it plays an indirect yet significant role in modifying the reaction environment. Through partial thermal decomposition at elevated temperatures, the oil undergoes fragmentation of its organic constituents, primarily fatty acids and glycerides, which generates an electron-rich atmosphere within the reaction medium. These decomposition products serve as electron donors, releasing free electrons that actively contribute to the reduction of vanadium species. In this way, the conversion of oxovanadium sulfate [$VO(SO_4)_2$] into vanadyl sulfate ($VOSO_4$) is facilitated [16]:

$$VO(SO_4)_2 + H_2O + e^- \rightarrow VOSO_4 + H_2SO_4 \quad (4)$$

When the reaction system is subjected to heating in the presence of olive oil, the organic matrix of the oil undergoes progressive thermal decomposition. This process generates carbonaceous by-products, including activated carbon, which possess a high surface area and notable reactivity. These carbon-derived materials actively participate in the reaction medium by improving the mobility and transfer of oxygen species, thus creating a more favorable environment for oxidation reactions.At elevated temperatures, the decomposition products of the oil—particularly the fragmented organic molecules—act as auxiliary oxygen carriers. By facilitating the transport and redistribution of oxygen within the system, they promote the effective oxidation of vanadium precursors. As a result, the transformation of vanadium into its highest oxidation state occurs, yielding vanadium pentoxide (V_2O_5). The overall oxidation pathway that illustrates this process is summarized by the chemical equation provided below:

$$VO(SO_4)_2 \rightarrow V_2O_5 + SO \quad (5)$$

The oil acts to minimize the formation of unwanted by-products while preserving a relatively clean environment during calcination.

3. RESULTS AND DISCUSSIONS

FTIR Analysis of Vanadyl Sulfate ($VOSO_4$)

Figure 1 illustrates the Fourier Transform Infrared (FTIR) spectrum of vanadyl sulfate ($VOSO_4$), highlighting the characteristic absorption features associated with its molecular structure. A broad band appearing around 3400 cm^{-1}, together with a distinct signal near 1645 cm^{-1}, can be ascribed to the stretching and bending vibrations of water molecules coordinated within the crystal lattice, confirming the presence of hydration in the compound. In addition,

two strong absorptions are clearly visible at approximately 1047 cm^{-1} and 983 cm^{-1}. These peaks are assigned to the stretching vibration of the sulfate group (S=O) and the terminal vanadyl bond (V=O), respectively, both of which are fundamental to the structural identity of $VOSO_4$. Furthermore, multiple absorption bands detected in the lower wavenumber region, specifically within the 650–450 cm^{-1} range, correspond to V–O and V–O–S vibrational modes. These modes provide further confirmation of the bonding environment and validate the expected molecular composition of the material, consistent with literature reports for hydrated vanadyl sulfate.

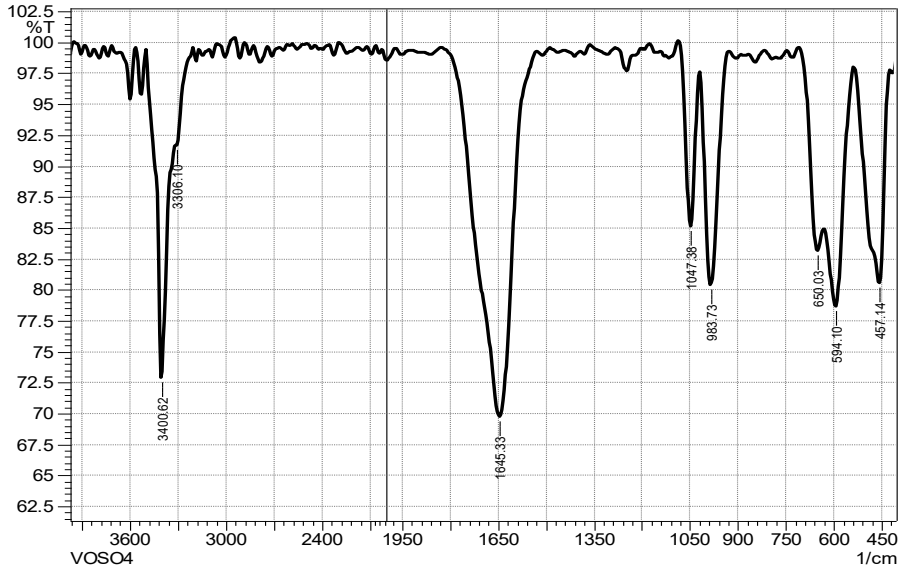

Figure 1. presents the Fourier-transform infrared (FTIR) spectrum of vanadium sulfate (V_2SO_4).

Infrared Spectroscopy Analysis (FTIR) of Virgin Olive Oil

Figure 2 displays the Fourier Transform Infrared (FTIR) spectrum of virgin olive oil, revealing several characteristic absorption bands that are indicative of its molecular composition. A strong and well-defined band appears at approximately 1743 cm^{-1}, corresponding to the stretching vibration of the ester carbonyl group (C=O), which arises from the triacylglycerol backbone that dominates the oil's structure. Distinct absorption peaks at 2928 cm^{-1} and 2867 cm^{-1} are associated with the asymmetric and symmetric stretching modes of aliphatic C–H bonds, characteristic of long hydrocarbon chains in fatty acids. In addition, a broad feature near 3498 cm^{-1} can be attributed to O–H stretching vibrations, which originate primarily from phenolic compounds and minor hydroxyl-containing constituents naturally present in virgin olive oil. Another diagnostic band appears at around 1464 cm^{-1}, assigned to the bending vibrations of methylene (CH_2) groups, further supporting the predominance of

long-chain aliphatic moieties. Taken together, these spectral features are in excellent agreement with values reported in the literature for edible-grade olive oil, thereby confirming the authenticity and chemical integrity of the analyzed sample.

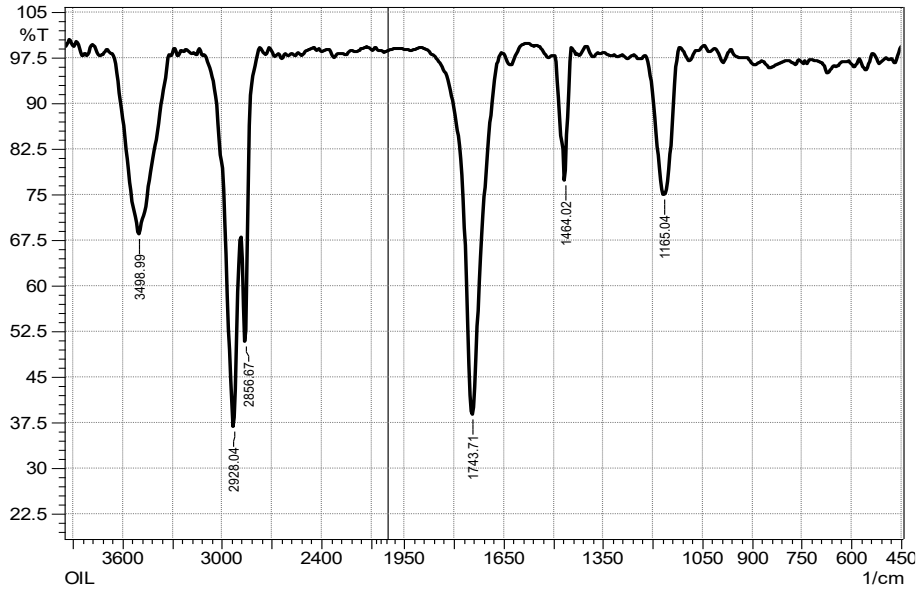

Figure 2. presents the Fourier-transform infrared (FTIR) spectrum of virgin olive oil.

Infrared Spectroscopy Analysis (FTIR) of V_2O_5

As illustrated in Figure 3, the FTIR spectrum of vanadium pentoxide (V_2O_5) reveals several characteristic vibrational bands that reflect its molecular and structural features. A prominent absorption near 1000 cm^{-1} corresponds to the stretching vibration of the terminal vanadyl bond (V=O), while another significant band observed around 816 cm^{-1} is attributed to the bridging V–O–V vibrations within the layered oxide framework. Additionally, broad absorption features centered at approximately 3402 cm^{-1} and 1622 cm^{-1} indicate the presence of water molecules physically adsorbed on the surface of the V_2O_5 particles. These bands arise from the stretching and bending vibrations of O–H groups, respectively, and suggest partial hydration or surface hydroxylation, which is commonly observed in vanadium pentoxide powders. Overall, the spectrum confirms the formation of V_2O_5 and provides insight into both its bonding environment and interaction with moisture.

Figure 3. presents the Fourier-transform infrared (FTIR) spectrum of vanadium pentoxide (V_2O_5).

X-ray Diffraction (XRD) of V_2O_5

The X-ray diffraction (XRD) pattern presented in Figure 4 exhibits a series of well-defined and sharp diffraction peaks at 2θ values of 20.5°, 26.3°, 31.3°, 32.6°, 34.5°, 41.5°, 45.7°, 47.8°, and 49.2°, which are characteristic of orthorhombic vanadium pentoxide (V_2O_5) and are in excellent agreement with the reference data (PDF 41-1426). The sharpness and intensity of these reflections indicate a highly ordered crystalline structure with minimal lattice defects. To further quantify the crystalline domain size, the Scherrer equation was applied to the most prominent peaks in the diffraction pattern. Based on this analysis, the average crystallite size of the synthesized V_2O_5 was estimated to be approximately 16.57 nm. This nanoscale dimension, combined with the high crystallinity inferred from the peak profiles, suggests that the material possesses a well-developed crystalline lattice suitable for applications requiring high surface reactivity and structural stability.

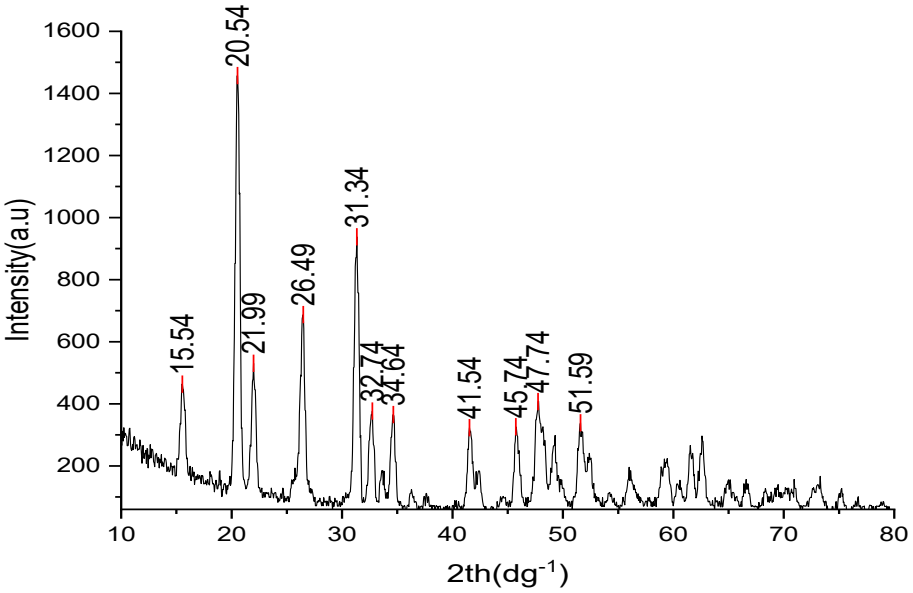

Figure 4. presents the X-ray diffraction (XRD) pattern of vanadium pentoxide (V_2O_5).

Field-emission SEM (FE-SEM) of V_2O_5

Figure 5 presents a representative field-emission scanning electron microscopy (FE-SEM) micrograph of the synthesized material, obtained using a MIRA3 TESCAN instrument operated at an accelerating voltage of 15.0 kV, with a working distance of 8.11 mm and a magnification of 350,000×. Imaging was performed using a secondary-electron detector, which provides high-resolution surface morphology information. The micrograph reveals that the sample consists of irregularly shaped nanoparticles with a relatively uniform distribution. Measurement of individual particles indicates an average diameter of approximately 32.62 nm, confirming the nanoscale nature of the synthesized vanadium oxide. Such nanoscale dimensions are particularly advantageous for applications that rely on high surface area and reactivity, including heterogeneous catalysis, electrode materials for batteries, gas sensing devices, and components in photovoltaic systems. The observed morphology and particle size are therefore consistent with the desired structural characteristics for these technologically relevant applications.

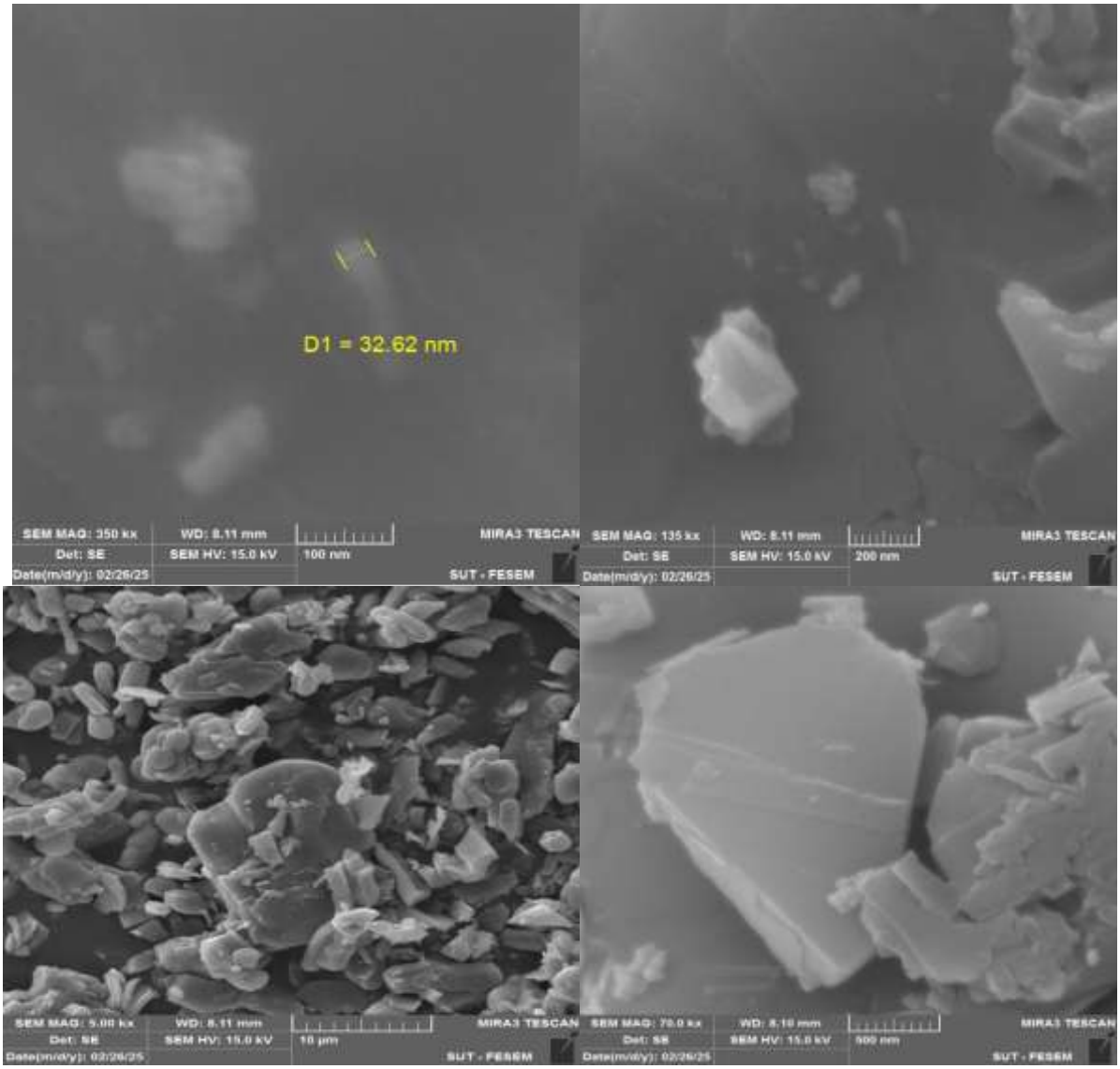

Figure 5. presents the field emission scanning electron microscopy (FE-SEM) images of vanadium pentoxide (V_2O_5).

Brunauer–Emmett–Teller (BET) and Barrett–Joyner–Halenda (BJH) Analyses

Nitrogen adsorption–desorption isotherms (Figure 6) yielded a BET surface area of 10.817 m^2/g and a total pore volume of 0.024277 cm^3/g. According to IUPAC classification, the isotherm features indicate heterogeneous porosity (mixed type IV/II behavior). The BJH pore-size distribution (Figure 7) spans ~20–90 nm. Table 1 summarizes the surface area and porosity parameters for the V_2O_5 sample.

Table 1. Parameters obtained from BET analysis of vanadium oxide.

Sample	Lag.specific surfacearea (m^2 g^{-1})	BET specific surfacearea (m^2 g^{-1})	Pore Volume (cm^3g^{-1})	Average pore diameter
V_2O_5	15.953	10.817	0.024277	8.9775

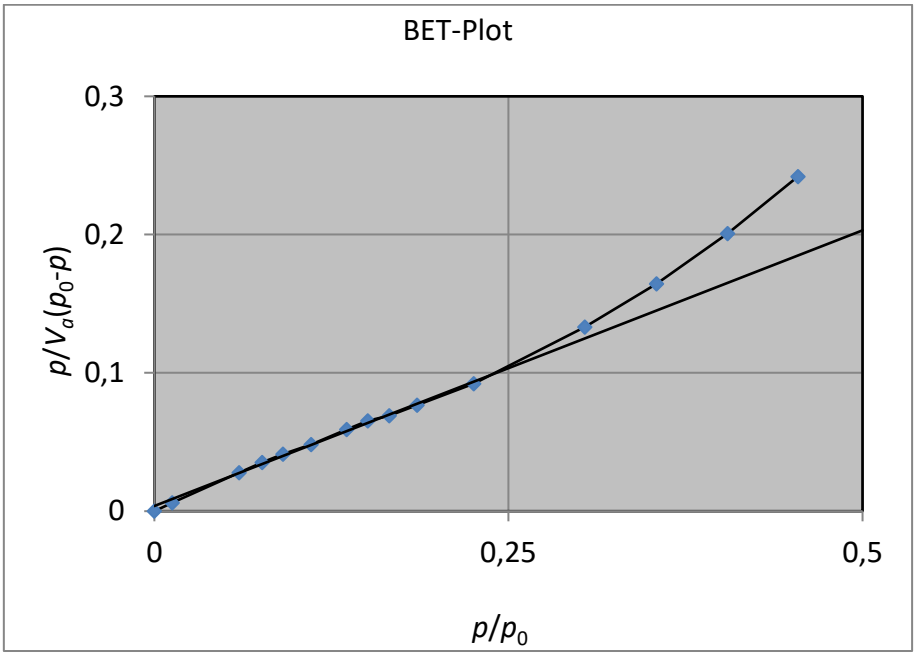

Figure 6. presents the Brunauer–Emmett–Teller (BET) analysis of vanadium pentoxide (V_2O_5).

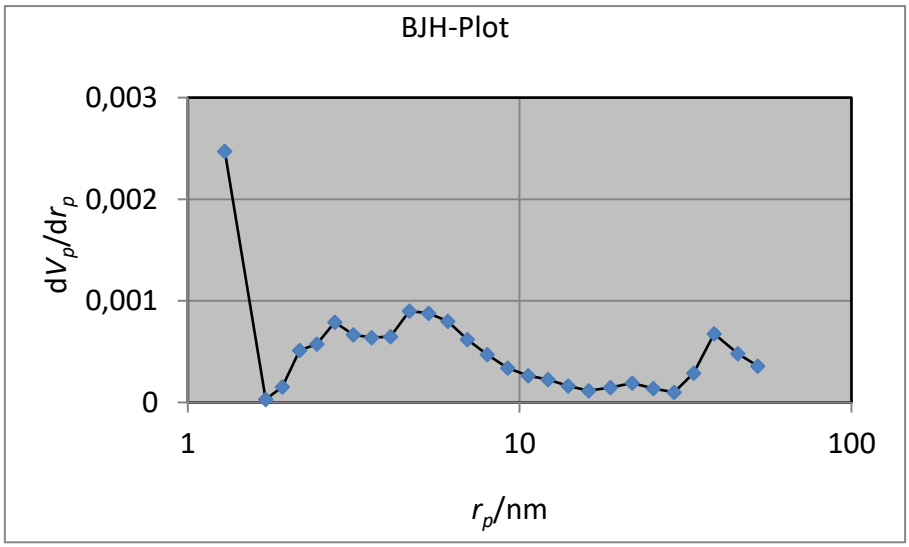

Figure 7. presents the Barrett–Joyner–Halenda (BJH) analysis of vanadium pentoxide (V_2O_5).

Dispersive X-ray Analysis (EDX) of V_2O_5

The EDX spectrum (Figure 8) confirms the elemental composition of vanadium and oxygen with weight fractions of ~69.40% V and ~30.60% O, consistent with stoichiometric V_2O_5.

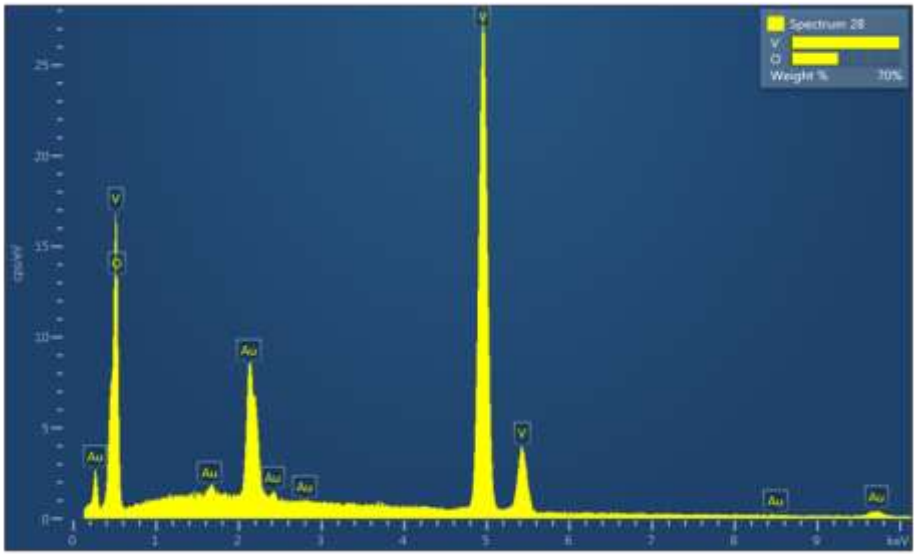

Figure 8. presents the energy-dispersive X-ray (EDX) spectrum of vanadium pentoxide (V_2O_5).

4. CONCLUSION AND DISCUSSION

Vanadium pentoxide (V_2O_5) nanoparticles were synthesized using a green chemistry approach with virgin olive oil as a natural reducing agent and catalyst. FESEM analysis revealed particles averaging 32.62 nm with slightly irregular shapes, reflecting the role of organic constituents in crystal growth. FTIR spectra showed O–H vibrations at 3402.45 and 1622.02 cm^{-1}, while V=O and V–O–V bonds appeared at 1000.27 and 815.83 cm^{-1}, confirming V_2O_5 formation with minor moisture. XRD analysis confirmed a pure crystalline structure with an average crystallite size of 16.57 nm. BET measurements indicated a surface area of 10.817 m^2/g and a pore volume of 0.024277 cm^3/g. EDX results showed vanadium and oxygen contents of 69.40% and 30.60%, respectively, consistent with the V_2O_5 formula. These characteristics suggest the material's suitability for applications in catalysis, energy storage, and sensing.

Declarations

Funding

Not applicable.

Conflicts of Interest/Competing Interests

The authors declare that they have no conflict of interest.

Ethics Approval and Consent to Participate

Not applicable.

Consent for Publication

Not applicable.

Availability of Data and Materials

The datasets generated and/or analyzed during the current study are available from the corresponding author on reasonable request.

Authors' Contributions

[Ahmed Saleh Yaseen] designed the study. [Yosef Othman Homeda] carried out the experiments. [Mohammad M. Al-Tufah, Mutlak Saud Khalaf, and Mohannd Faisal Shareef] analyzed the data. All authors read and approved the final manuscript.

REFERENCE

Aimbetova, I., Jimenez-Castaneda, R., Clavijo-Blanco, J., Umirov, B., & Seitov, B. (2023). Investigation of optical and physico-chemical properties of titanium-doped V_2O_5 nanofilms. *Complex Use of Mineral Resources, 325*(2), 47–52. https://doi.org/10.31643/2023/6445.17

Ajeya, K. V., Sadhasivam, T., Kurkuri, M. D., Kang, U. I., Park, I. S., Park, W. S., Kim, S. C., & Jung, H. Y. (2020). Recovery of spent $VOSO_4$ using an organic ligand for vanadium redox flow battery applications. *Journal of Hazardous Materials, 399*, 123047. https://doi.org/10.1016/j.jhazmat.2020.123047

Aswini, K., Munirathnam, K., Manjunath, V., Reddy, N. N. K., Alhammadi, S., Kumar, K. S., Golkonda, S. R., Minnam Reddy, V. R., Kim, W. K., Ranjith, R., & Amina, M. (2025). Enhanced microstructure and electrical performance of a cost-effective Ni/Cu/n-GaN Schottky diode with a V_2O_5 interlayer for optoelectronic applications. *Journal of Materials Science: Materials in Electronics, 36*(7), 430. https://doi.org/10.1007/s10854-025-14466-y

Azimi, Y., Hosseini, M. R., Azimi, E., & Pedram, H. (2024). Comparison of enhanced neural network and response surface models in predicting bio-dissolution of aluminum and vanadium. *Journal of the Taiwan Institute of Chemical Engineers*. https://doi.org/10.1016/j.jtice.2024.105685

Boni, M., Bouabdellah, M., Boukirou, W., Putzolu, F., & Mondillo, N. (2023). Vanadium ore resources of the African continent: State of the art. *Ore Geology Reviews, 157*, 105423. https://doi.org/10.1016/j.oregeorev.2023.105423

Cestarolli, D. T., & Guerra, E. M. (2021). Vanadium pentoxide (V_2O_5): Obtaining methods and applications. In *Transition metal compounds: Synthesis, properties, and application* (p. 27). IntechOpen. https://doi.org/10.5772/intechopen.96860

Ch, S. L., Sameera, M., Jayasree, M., Kamala, G., & Degala, R. P. (2025). A review of industrial applications of green chemistry. *Journal of Pharma Insights and Research, 3*(1), 186–196. https://doi.org/10.69613/der2my50

Chauhan, P. S., Kumar, S., Mondal, A., Sharma, P., Parekh, M. N., Panwar, V., Rao, A. M., & Misra, A. (2023). Stacked vanadium pentoxide–zinc oxide interface for optically chargeable supercapacitors. *Journal of Materials Chemistry A, 11*(1), 95–107. https://doi.org/10.1039/D2TA06790K

Gao, Y., Remón, J., & Matharu, A. S. (2021). Microwave-assisted hydrothermal treatments for biomass valorisation: A critical review. *Green Chemistry, 23*(10), 3502–3525. https://doi.org/10.1039/D1GC00623A

Gardeli, C., Sykioti, S., Exarchos, G., Koliatsou, M., Andritsos, P., & Panagou, E. Z. (2025). Differentiation of extra virgin olive oil from other olive oil categories based on FTIR spectroscopy and random forest. *Applied Sciences, 15*(3), 1061. https://doi.org/10.3390/app15031061

Gnanasekar, S., & Nirmala Grace, A. (2022). V_2O_5 nanosheets as an efficient, low-cost Pt-free alternate counter electrode for dye-sensitized solar cells. *ChemNanoMat, 8*(2), e202100382. https://doi.org/10.1002/cnma.202100382

Hu, P., Hu, P., Vu, T. D., Li, M., Wang, S., Ke, Y., Zeng, X., Mai, L., & Long, Y. (2023). Vanadium oxide: Phase diagrams, structures, synthesis, and applications. *Chemical Reviews, 123*(8), 4353–4415. https://doi.org/10.1021/acs.chemrev.2c00546

Kamali, S., Esfandyari, M., & Jafari, D. (2025). A review of the application of polymeric materials in microbial fuel cells. *Polymer Bulletin*, 1–28. https://doi.org/10.1007/s00289-025-05792-6

Kaur, J., & Kumar, R. (2025). Rapid dye removal using MoO_3-incorporated V_2O_5 nanocomposites: Laboratory experiments and real-world applications. *SSRN Electronic Journal*. https://doi.org/10.2139/ssrn.5245116

Le, D. N., Le, T. A., Le, T. P. H., Dang, C. M., Tu, P. H., Shiratori, Y., & Doan, T. C. D. (2025). Morphology evolution of Fe-doped V_2O_5 flower-like microspheres for H_2S adsorption. *Materials Chemistry and Physics, 335*, 130541. https://doi.org/10.1016/j.matchemphys.2025.130541

Nguyet, T. T., Van Duy, L., Nam, N. C., Dat, D. Q., Nguyen, H., Hung, C. M., Van Duy, N., & Hoa, N. D. (2025). Transition from p-type to n-type semiconductor in V_2O_5 nanowire-based gas sensors: Synthesis and sensing mechanism. *Sensors and Actuators B: Chemical, 424*, 136841. https://doi.org/10.1016/j.snb.2024.136841

Roznyatovskaya, N. V., Fühl, M., Roznyatovsky, V. A., Noack, J., Fischer, P., Pinkwart, K., & Tübke, J. (2020). Influence of free acid in vanadium redox-flow battery electrolyte on power drop effect and thermally induced degradation. *Energy Technology, 8*(10), 2000445. https://doi.org/10.1002/ente.202000445

Sohaimi, K. S. A., Jaafar, J., & Rosman, N. (2023). Synthesis, properties, and applications of vanadium pentoxide (V_2O_5) as photocatalyst: A review. *Malaysian Journal of Fundamental and Applied Sciences, 19*(5), 901–914. https://doi.org/10.11113/mjfas.v19n5.2774

Son, Y., Song, S., Lee, D., Han, S., Lee, J., Kwon, S., Jeon, J., Bae, J. S., Kim, H. H., Kang, H., & Park, S. (2025). In situ electrical resistance monitoring of vanadium oxide

reduction. *Journal of Alloys and Compounds*, 180705. https://doi.org/10.1016/j.jallcom.2025.180705

Tong, C. (2025). Flexible zinc-ion batteries. In *Advanced energy materials for flexible batteries* (pp. 181–229). Springer Nature Switzerland. https://doi.org/10.1007/978-3-031-83971-9_6

Wang, Z., Chen, L., Yin, R., Li, Z., Deng, G., Liang, B., Zhu, Y., Wu, K., & Luo, D. (2023). Preparation of vanadyl sulfate electrolyte for vanadium flow battery from vanadium slag. *Hydrometallurgy, 222*, 106146. https://doi.org/10.1016/j.hydromet.2023.106146

Wei, L., Hou, H., Wang, J., Chen, Y., Chen, Y., Chen, R., & Li, R. (2025). Preparation of vanadium flow battery electrolytes: In-depth analysis and prospects. *Ionics*, 1–10. https://doi.org/10.1007/s11581-025-06498-5

Zhang, X., Zhang, Z., Xu, S., Xu, C., & Rui, X. (2023). Advanced vanadium oxides for sodium-ion batteries. *Advanced Functional Materials, 33*(49), 2306055. https://doi.org/10.1002/adfm.202306055